
Analog Integrated Circuits and Signal Processing, 28, 279–291, 2001

A Current-Mode Hysteretic Winner-take-all Network, with Excitatory and Inhibitory Coupling

GIACOMO INDIVERI

Institute of Neuroinformatics, University/ETH Zürich
E-mail: giacomo@ini.phys.ethz.ch

Received February 3, 2000; Revised August 24, 2000; Accepted December 8, 2000

Abstract. Winner-take-all (WTA) circuits are commonly used in a wide variety of applications. One of the most used current-mode WTA designs is the one originally proposed by Lazzaro et al. [1]. Several extensions to this design have been suggested in the past. In this paper we present a variant of this current-mode WTA circuit, containing all of the enhancements previously proposed, together with new additional modifications that endow it with interesting hysteretic and lateral inhibition and excitation properties. We compare the performance of this WTA circuit to the original WTA design, providing experimental data obtained from a VLSI chip containing both types of circuits, designed using closely matched layouts. We derive analytically the response properties of the circuit's lateral diffusion network, pointing out the differences to previously proposed diffusion networks, and present experimental data confirming the theoretical predictions. We also describe application domains that can best exploit these types of hysteretic WTA circuits.

Key Words: neuromorphic circuits, analog VLSI, winner-take-all, diffusor network

1. Introduction

CMOS implementations of winner-take-all (WTA) networks are an important class of circuits widely used in neural networks and pattern-recognition systems. They implement architectures that select one node, out of many, through a competition mechanism that depends on the amplitude of the architecture's input signals. Several types of WTA circuits have been proposed in the literature [1–10]. Each WTA circuit was designed with specific optimization constraints in mind. For example, the circuits proposed in [2] and in [8] are optimal for high-speed, high-precision applications, whereas the circuits of [6] and [7] are optimal for pulse-coded neural networks. The WTA circuit proposed by Lazzaro et al. [1] optimizes power consumption and silicon area usage. It is ideal for applications that do not require high precision or high speed computation, such as sensory perception tasks [11–13]. This circuit, proposed more than ten years ago, still remains one of the most compact and elegant designs of analog current-mode WTA circuits. It is asynchronous; it responds in real-time; and it processes all its input currents in parallel, using only two transistors per node, if the output signal is a voltage, and four transistors if the output signal is a current (see Fig. 1(b)). Recently, some extensions to the basic design described in [1] have been proposed [14–16]. They endow the WTA circuit with local excitatory feedback [14] and with distributed hysteresis [15,16]. Local excitatory feedback enhances resolution and speed performance of the circuit, providing a hysteretic mechanism that withstands the selection of other potential winners unless they are stronger than the selected one by a set hysteretic current. Distributed hysteresis allows the winning input to shift between adjacent locations maintaining its winning status, without having to reset the network. These enhanced types of WTA networks are able to select and lock onto the input with strongest amplitude, and to track it as it shifts smoothly from one pixel to its neighbor [17–19].

In this paper we propose a new version of the current-mode WTA circuit that contains local excitatory feedback and lateral excitatory coupling (to implement distributed hysteresis) but that also implements lateral inhibitory coupling and diode-source degeneration. The interactions between the non-linearities of the WTA network and the lateral coupling networks produce center-surround spatial response properties that

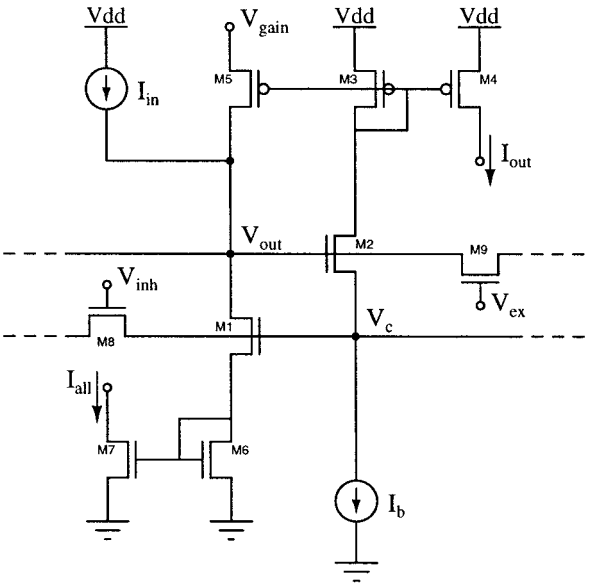

Fig. 1. (a) Hysteretic WTA cell, with local excitatory feedback, lateral excitatory coupling, lateral inhibitory coupling and diode-source degeneration. (b) Basic current-mode WTA cell.

differ from the ones obtained using conventional spatial diffusion networks [20,21]. To make an accurate comparison between the performance of the new WTA network and the performance of the classical WTA network described in [1], we implemented both circuits on the same chip, using transistors of the same size, common bias pads and the same input sources. In the next two sections we describe the circuits, present experimental data from both networks, derive analytically the hysteretic WTA network's lateral coupling properties as a function of the circuit parameters, point out the differences to conventional diffusor networks and show the response properties of the circuit when both lateral excitatory and lateral inhibitory couplings are enabled. Finally in Section 4 we suggest possible application domains for the type of network proposed, and in Section 5 we make some concluding remarks.

2. The WTA Circuit

The circuit diagram of one cell of the hysteretic WTA network proposed in this paper is shown in Fig. 1(a). Fig. 1(b) shows the original current-mode WTA network, as originally proposed in [1], for comparison. We implemented both circuits on the same chip, using a 2 μm CMOS technology, as linear arrays of 25 cells. The cell size of the hysteretic WTA network is 60 μm $\times$ 100 μm. To minimize device mismatch effects, the layout of the classical WTA circuit was designed to be as similar as possible to the layout of the hysteretic WTA circuit. For this reason the cell of the classical WTA network, though less dense, also measures 60 μm $\times$ 100 μm.

The current source shown in Fig. 1 that generates the bias current I_b can be implemented using a single n-type MOS transistor. If the transistor operates in weak-inversion (or *subthreshold*), the amplitude of the bias current I_b depends exponentially on its gate voltage V_b [22]. In this regime the transistor is in saturation as long as $V_c \geq 4U_T$ (i.e., $V_c \geq 100$ mV), its output current being: $I_b = I_0 e^{\frac{\kappa V_b}{U_T}}$. The term U_T represents the thermal voltage, I_0 the zero bias current, and κ the subthreshold slope coefficient [22]. In practical applications I_b can be set by providing an external bias current into a single diode-connected transistor that has its gate connected to all the network's bias transistors (thus implementing a series of current-mirrors). Similarly, the input current source that generates I_{in} can be

implemented using a p-type transistor operating in the subthreshold regime. Although the WTA circuit can operate both in the weak and strong inversion regimes, it is typically operated in the weak inversion/subthreshold regime. In this regime the circuit is particularly sensitive to device mismatch and noise. In the existent implementation, when operated in subthreshold the circuit selects one single winner if its input currents differ by at least 10%. The low currents provided by the subthreshold input transistors and by the bias transistor (typically ranging from fractions of pico-Amperes to hundreds of nano-Amperes) also limit the circuit's dynamic response properties. As with the original WTA circuit, the network's time constant is dominated by the maximum input current and ranges from fractions of milliseconds up to fractions of seconds. The detailed, quantitative analysis of the WTA's dynamic response properties discussed in [1] is valid also for the circuit proposed in this paper. As the original WTA circuit, this circuit is ideal for tasks that do not rely on high precision and do not require time constants lower than a few milliseconds. Fortunatelly, most applications involving perception and processing of sensory signals fall into this category. Examples of applications of this kind are provided in Section 4.

The main differences between the original WTA design and the one described here are implemented by transistors M5 through M9, as shown in Fig. 1. Specifically, transistor M5, together with M3 of Fig. 1(a) implement *local excitatory feedback*. Transistor M6 implements *diode-source degeneration,* and transistors M8 and M9 implement inhibitory and excitatory *lateral coupling*.

2.1. Local Excitatory Feedback

The main effect of local excitatory feedback is to introduce a hysteretic behavior into the WTA network. Once a cell is selected as the winner, a current proportional to the network's bias current I_b is sourced back into the cell's input node through the current-mirror formed by M3 and M5 (see Fig. 1(a)). If the bias current I_b is a subthreshold current, the proportionality factor of the local excitatory feedback current is modulated exponentially by the voltage difference $(V_{dd} - V_{gain})$. Hysteresis is evident because, after a cell has been selected as the winner, to lose its winning status the cell's input current has to decrease by an additional amount equal to the local excitatory feedback current. Fig. 2 shows the output of a cell of the hysteretic WTA network, superimposed on the output of the corresponding cell belonging to the classical WTA network, in response to the same input signals. For both types of WTA networks, input currents were applied only to two neighboring cells, while all other cells received no input. The common mode input current of the stimulated cells was set by biasing the input p-type transistors with a constant voltage $V_{in} = 4.2$ V. The bias current of both WTA networks was generated using a bias voltage $V_b = 0.67$ V. The local excitatory feedback loop of the hysteretic WTA circuit was fully activated ($V_{gain} = V_{dd}$). The width of the hysteresis curve can be modulated by changing either the WTA network's bias current I_b, or the control voltage V_{gain}.

The stability properties of the hysteretic WTA network are the same as those of conventional winner-take-all circuits with positive feedback, and have been analyzed in detail in [14]. Similarly, the dynamic response properties of the hysteretic WTA network are the same as those of the classical current-mode WTA network described in [1] and depend mainly on the values of I_b and of the total current entering the input nodes of the WTA cells.

2.2. Diode-source Degeneration

Source degeneration, also referred to as emitter degeneration for bipolar transistors, is a classical technique in analog design [23]. It consists of converting the current flowing through a transistor into a voltage, by dropping it across a resistor or a diode, and feeding this voltage back to the source of the transistor, to increase its gate voltage accordingly. At the WTA network level, source degeneration of the input transistor has the effect of increasing the circuit's winner selectivity gain. This is evident in Fig. 3, where the output of the diode-source degenerated network is superimposed on the output of the classical WTA network, in response to the same input signals. This figure shows the output of four cells (two neighboring cells per type of WTA network) as they change their state from winning to losing and vice-versa. Small differences in the amplitude of the winning signals are due to mismatches of the readout transistors (M4 of Fig. 1(a)). The data was taken using the same input stimulus arrangement described for Fig. 2. The bias current of both WTA networks was generated using a bias voltage $V_b = 0.7$ V. Local excitatory feedback (and the hysteretic behavior associated with

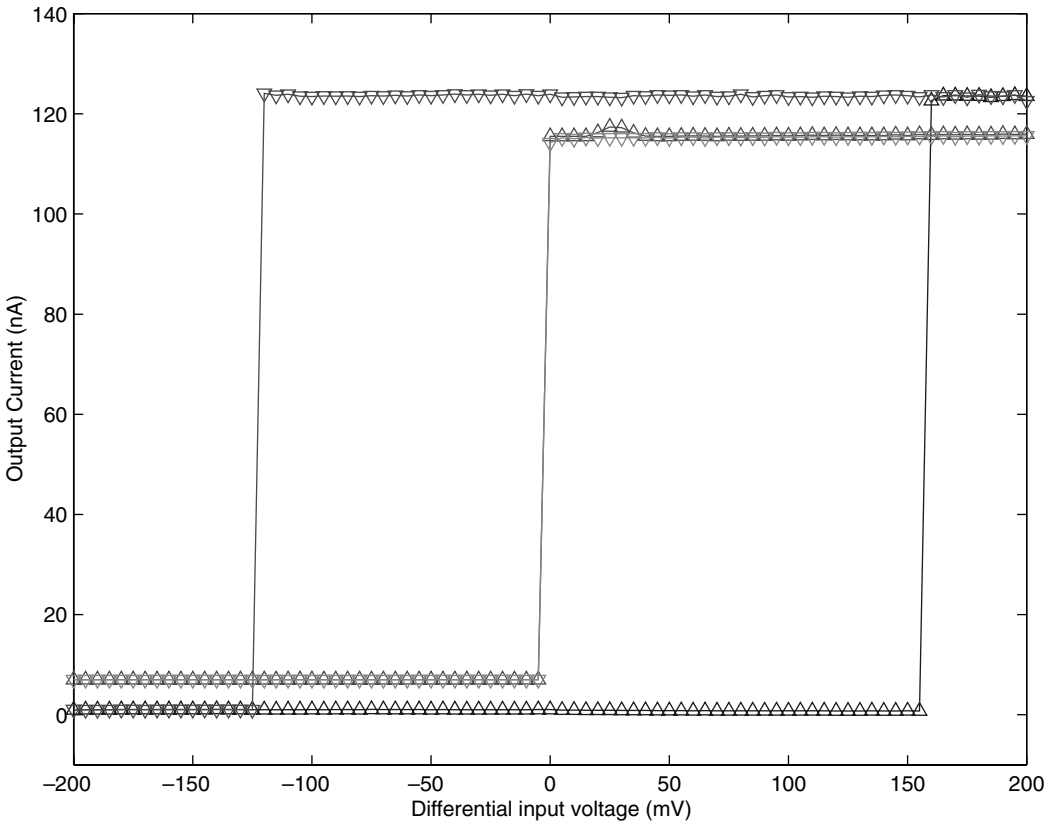

Fig. 2. Response of the hysteretic WTA circuit (outer hysteresis plot) superimposed to the response of the classical WTA circuit (inner central plot). The output of the classical WTA circuit was shifted vertically by a few nano-amperes for sake of clarity.

it) was disabled by setting the control voltage V_{gain} to 3 V.

By adding just one transistor and connecting its gate to the diode-source degeneration transistor of each WTA cell (see M7 of Fig. 1) it is possible to read out a copy of the cell's net input current I_{all}. As I_{all} represents the sum of all of the currents converging into the WTA cell (namely, the input current I_{in}, the current being spread to or from the left and right nearest neighbors and the local excitatory feedback current coming from the top p-type current mirror), it is a useful measure for visualizing the state of the WTA network.

3. Lateral Coupling

Lateral coupling is implemented in the hysteretic WTA network proposed here by means of "diffusor" (or "pseudo-conductance") networks [20,21]. Diffusor networks are extensively used in silicon retinas and other types of neuromorphic circuits. In the circuit proposed in this article the current diffusors are implemented by transistors M8 and M9 of Fig. 1(a), operated in the subthreshold regime. Specifically, transistor M9 implements lateral excitatory coupling and transistor M8 lateral inhibitory coupling. Functionally, the inhibitory diffusor network can be used to spatially decouple the WTA cells, while the excitatory diffusor network can be used to smooth the input signals, combined with the local excitatory feedback current of the winning cell (see Section 2.1).

3.1. Lateral Excitation

To study analytically the principle of operation of the excitatory diffusor network let us neglect, for the time being, the inhibitory diffusor network (i.e., let us set the inhibition to be global with $V_{inh} = 5$ V).

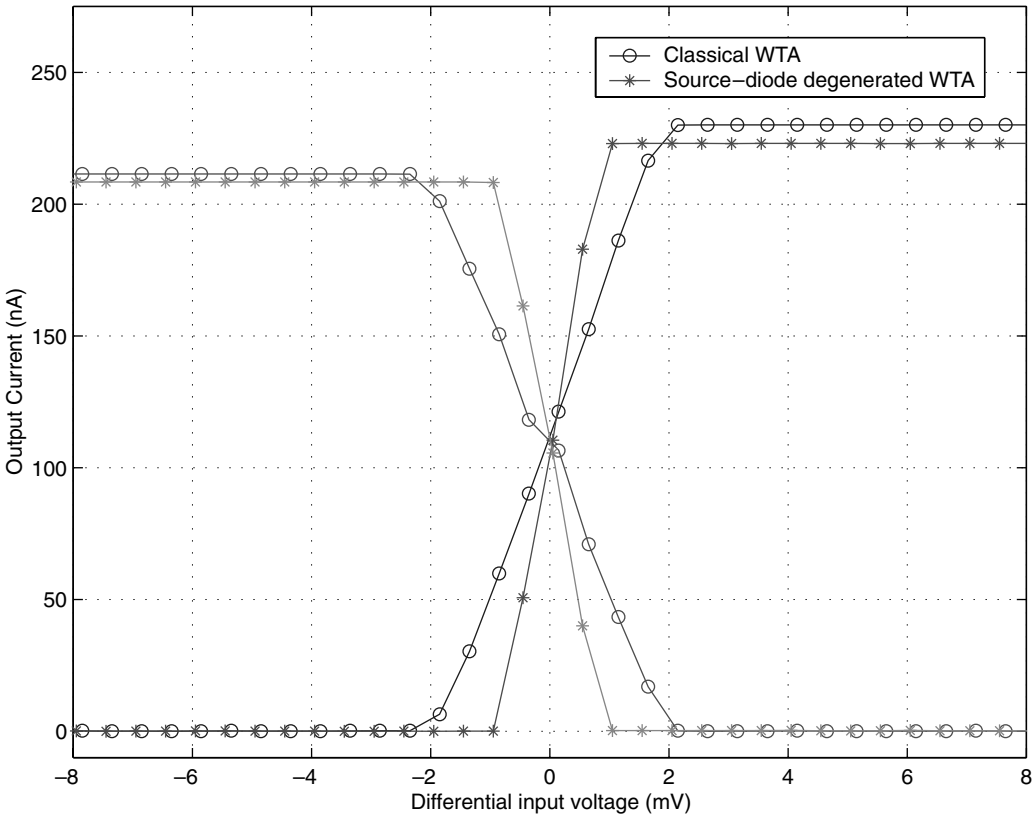

Fig. 3. Diode-source degenerated WTA network output and classical WTA network output.

Furthermore let us neglect, for the sake of simplicity, transistors M5, M6, and M7 of Fig. 1(a) and apply a constant subthreshold input current I_{in} only to the first node of the network. In this case the hysteretic WTA network reduces to the circuit shown in Fig. 4.

As pointed out by the figure, the (subthreshold) currents flowing through the diffusors can be separated into forward and reverse components: $I_{d,i} = I_{f,i} - I_{r,i}$, where

$$I_{r,i} = I_0 e^{\kappa \frac{V_{ex}}{U_T} - \frac{V_i}{U_T}} \tag{1}$$

$$I_{f,i} = I_0 e^{\kappa \frac{V_{ex}}{U_T} - \frac{V_{i+1}}{U_T}} \tag{2}$$

From these equations the following relationship holds:

$$I_{f,i} = I_{r,i+1} \tag{3}$$

By writing Kirchhoff's current law at each node i we have:

$$I_{a,i} = (I_{f,i-1} - I_{r,i-1}) - (I_{f,i} - I_{r,i}) \tag{4}$$

which, using equation (3), turns into:

$$I_{a,i} = 2I_{r,i} - I_{r,i-1} - I_{r,i+1} \tag{5}$$

but, if $I_{a,i}$ is a subthreshold current, we can also write:

$$I_{a,i} = I_0 e^{\kappa \frac{V_c}{U_T}} \left(1 - e^{-\frac{V_i}{U_T}}\right) \tag{6}$$

and, by expressing V_i in terms of $I_{r,i}$ (using equation (1))

$$I_{a,i} = I_0 e^{\kappa \frac{V_c}{U_T}} - e^{\kappa \left(\frac{V_c}{U_T} - \frac{V_{ex}}{U_T}\right)} I_{r,i} \tag{7}$$

which yields

$$I_{r,i} = \lambda I_0 e^{\kappa \frac{V_c}{U_T}} - \lambda I_{a,i} \tag{8}$$

where $\lambda = e^{-\kappa \left(\frac{V_c}{U_T} - \frac{V_{ex}}{U_T}\right)}$.

Substituting equation (8) into equation (5) we obtain the discrete approximation of a Laplacian:

$$I_{a,i} = \lambda(I_{a,i-1} - 2I_{a,i} + I_{a,i+1}) \tag{9}$$

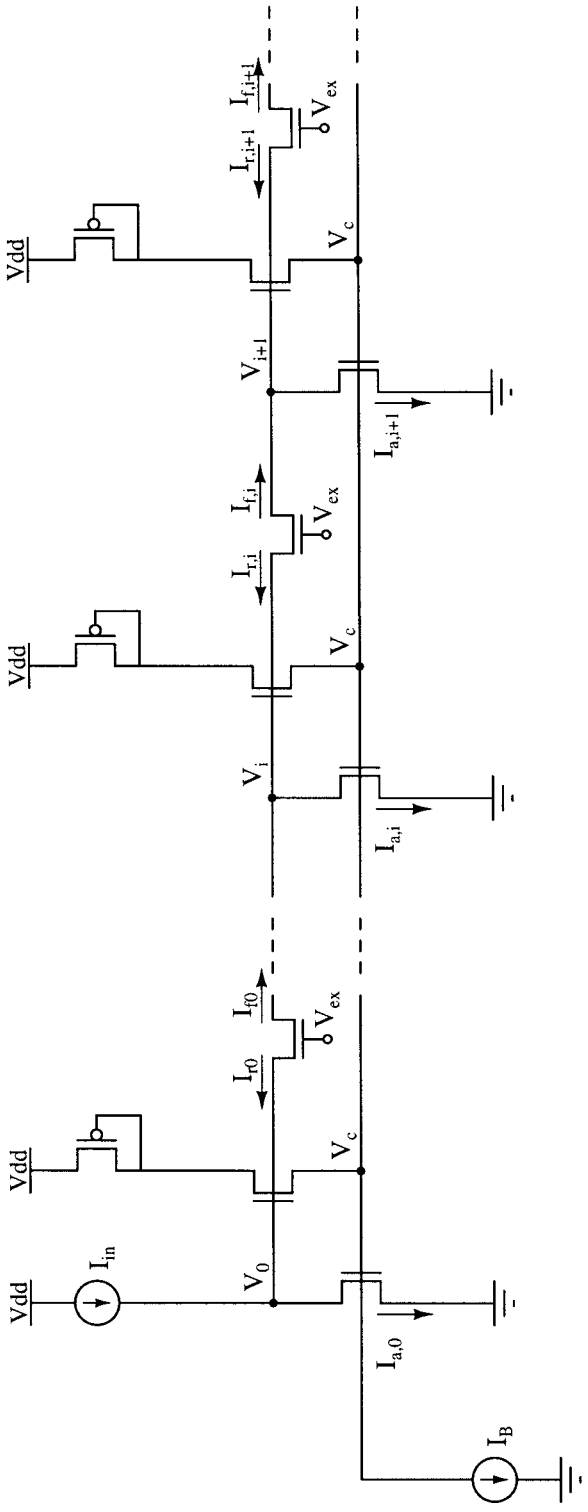

Fig. 4. Equivalent WTA circuit, used to analyze the excitatory diffusor network.

It follows that

$$I_{a,i} = \frac{\lambda}{1+2\lambda} I_{a,i-1} + \frac{\lambda}{1+2\lambda} I_{a,i+1} \quad (10)$$

By using this equation recursively we can write

$$I_{a,i} = \frac{\lambda}{1+2\lambda} I_{a,i-1} + \frac{\lambda^2}{(1+2\lambda)^2} (I_{a,i} + I_{a,i+2}) \quad (11)$$

If $\lambda \ll 1$, equation (11) reduces to

$$I_{a,i} \approx \lambda I_{a,i-1} \quad (12)$$

If we want to estimate the current flowing to ground through the nth transistor of the network $I_{a,n}$, we can use equation (12) recursively until we reach the first cell of the network (node 0):

$$I_{a,n} = I_{a,0} \lambda^n \quad (13)$$

but, as $I_{a,0} \approx I_{in}$ (if $\lambda \ll 1$), we can write:

$$I_{a,n} = I_{in} e^{-n\kappa \left(\frac{V_c}{U_T} - \frac{V_{ex}}{U_T} \right)}. \quad (14)$$

The term λ is defined as the network's *space constant*. The space constant (and with it, the network's spatial coupling) is modulated exponentially by the term $-(V_c - V_{ex})$. While V_{ex} is a directly accessible circuit parameter, independent of other circuit parameters, the voltage V_c depends logarithmically on the input current. Specifically, for the circuit of Fig. 4:

$$I_{a,0} = I_0 e^{k \frac{V_c}{U_T}} \approx I_{in} \quad (15)$$

With this relationship in mind, we can rewrite λ as a function of V_{ex} and I_{in}, and equation (13) reduces to:

$$I_{a,n} = I_{in} \left(\frac{I_0 e^{\kappa \frac{V_{ex}}{U_T}}}{I_{in}} \right)^n \quad (16)$$

According to this finding, an increase in V_{ex} will increase (exponentially) the amount of spreading and allow more current to flow through the diffusors. Conversely, increases in the amplitude of I_{in} will narrow the spreading width of the network and diminish the amount of current flowing through the diffusors. In this respect this excitatory diffusor network differs from the diffusor networks previously proposed [20] which have the undesirable property of increasing lateral spreading with increasing amplitude of input signals. In typical applications of diffusor networks, increasing the range over which spatial averaging takes place can be an effective strategy if the signal-to-noise ratio of the input signals is not too high. On the other hand, if input signals are strong, smoothing over large regions not only might not be useful, but could even be counterproductive. The experimental data of Fig. 5 confirms the theoretical predictions of equation (16). In Fig. 5(a) we stimulated the first cell of the hysteretic WTA network with a constant current and measured its response for different values of V_{ex}. As for the theoretical analysis, lateral inhibition is set to be global ($V_{inh} = 5$ V); the effects of the diode-source degeneration transistors can be neglected, as the currents flowing through the diode-connected transistors (M6 of Fig. 1(a)) are of the order of a few nano-amperes. The discontinuity present in the response profile between the first cell of the network and the second is due to the non-linear nature of the WTA competitive mechanism. From the second cell on, the measured current decays exponentially with distance, as predicted by equation (16), (see inset of Fig. 5(a)). In Fig. 5(b) we stimulated the first cell of the network with currents of increasing amplitude (for a fixed value of V_{ex}), measured the network's response and plotted the data on a normalized scale. As predicted by equation (16), and as shown in Fig. 5(b), lateral spreading *decreases* with *increasing* amplitude of the input current.

3.2. *Local Inhibition*

The local inhibitory diffusor network is equivalent in all respects to the local excitatory network. It can be shown, using the same methodology used to analyze the excitatory diffusor network, that the inhibitory diffusor network's space constant depends exponentially on I_{in} and on V_{inh}. We can see intuitively how V_{inh} allows us to modulate the spatial extent over which the WTA cells compete. In one extreme case inhibition is global (i.e., $V_{inh} = 5$ V), and the WTA network allows only one winner to be active at a time. In the other extreme case, the cells of the WTA network are completely decoupled from each other ($V_{inh} = 0$), and all cells are allowed to be simultaneously selected as winners. For intermediate values of V_{inh} the network can be biased to allow multiple winners to be active simultaneously, as long as they are sufficiently distant from each other.

Combining the effects of both excitatory and inhibitory networks, we can bias the hysteretic WTA network to exhibit different functional behaviors. Fig. 6 shows a comparison between the behavior of the clas-

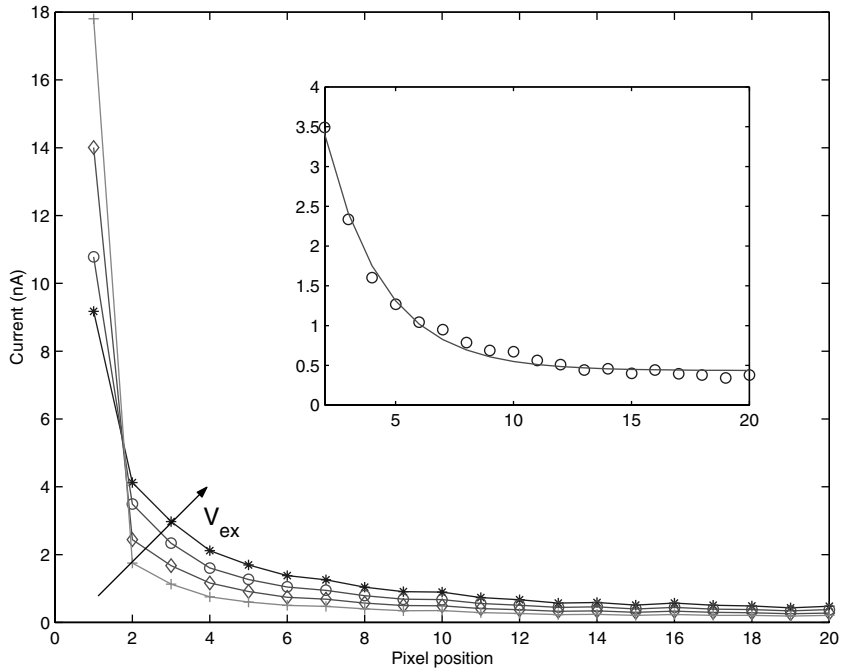

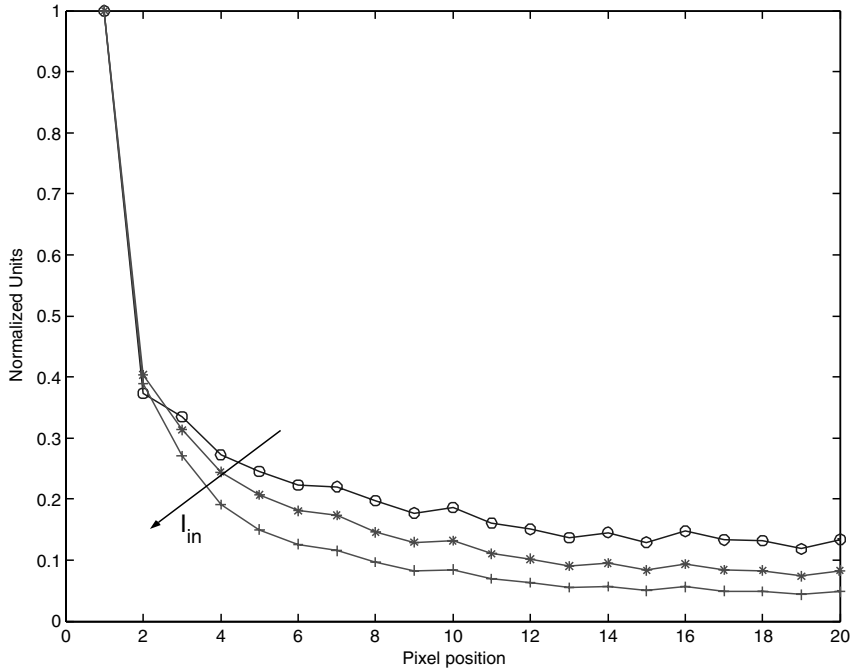

Fig. 5. Effect of lateral excitatory coupling on the hysteretic WTA network. (a) Output currents I_{all} (see Fig. 1(a)) measured at each pixel of the network for four increasing values of V_{ex}. The inset shows a fit of the data from pixel 2 to 20 with an exponential function. (b) Output currents I_{all} measured for three increasing values of I_{in}. Each data set is normalized to the maximum measured current.

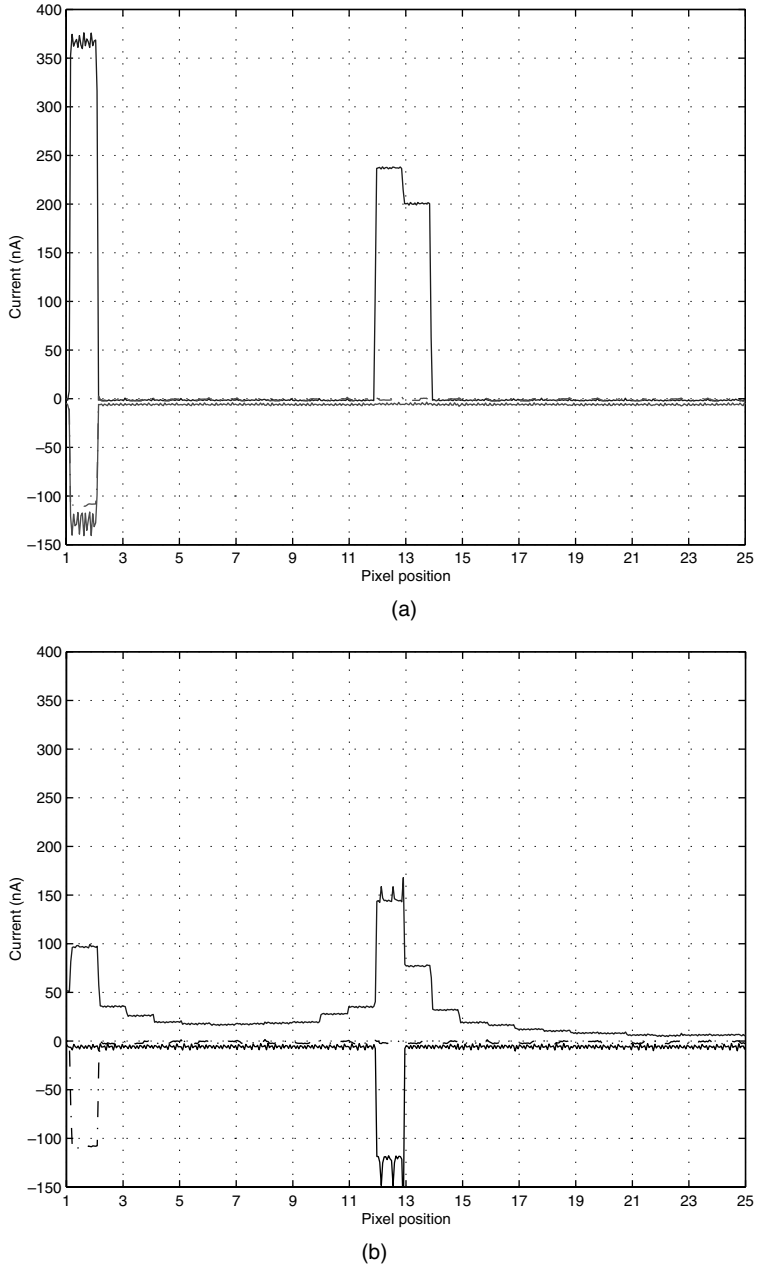

Fig. 6. Scanned output currents of hysteretic WTA network state (top solid-line), of hysteretic WTA output (bottom solid-line) and of classical WTA output (bottom dotted line). (a) Input currents are applied to pixel 1 ($V_{gs,1} = 1.1$ V), pixel 12 ($V_{gs,12} = 1.0$ V) and pixel 13 ($V_{gs,13} = 1.0$ V), lateral excitation is turned off ($V_{ex} = 0$ V) and inhibition is global ($V_{inh} = 5$ V). Both the basic WTA network and the hysteretic WTA network select pixel 1 as the winner. (b) Input signals and network bias settings are the same as in (a), but lateral excitation is turned on ($V_{ex} = 1.825$ V). The basic WTA network keeps on selecting the strongest absolute input as the winner (pixel 1), but the hysteretic WTA network selects the region with two neighboring pixels on, because it has a stronger *mean* activation. The total current entering pixel 12 is higher than the one entering pixel 13 due to the local excitatory feedback current. (c) Input currents are applied to pixels 5, 12 and 16 ($V_{gs,5} = 1.2$ V, $V_{gs,12} = 1.1$ V, $V_{gs,16} = 1.0$ V), lateral excitation is turned off and inhibition is global ($V_{ex} = 0$ V, $V_{inh} = 5$ V). Both the basic WTA network and the hysteretic WTA network select pixel 5 as the winner. (d) Input signals and network bias settings are the same as in (c), but inhibition is local ($V_{inh} = 3.35$ V). If inhibition is not global, the hysteretic WTA network allows *multiple* winners to be selected, as long as they are spatially distant (note that pixel 16 is selected as local winner, despite pixel 12 receives a stronger input current).

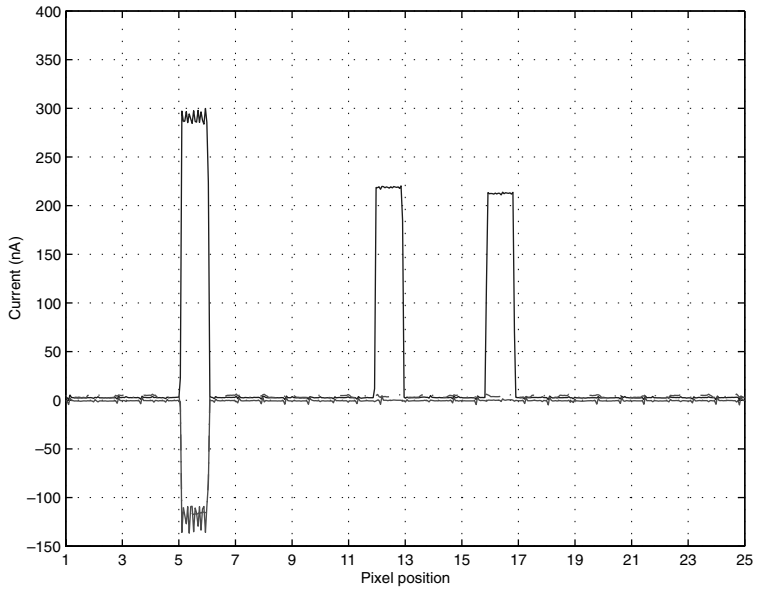

(c)

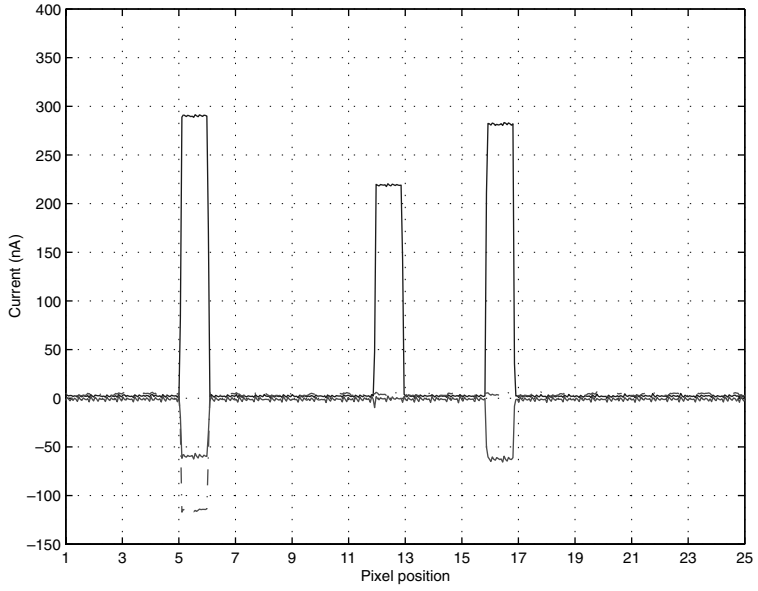

(d)

Fig. 6. (*Continued*)

sical WTA network and the behavior of the hysteretic WTA network for different input distributions and different settings of V_{ex} and V_{inh}.

Fig. 7 shows perhaps one of the most interesting response profiles that can be obtained combining lateral excitation and local inhibition in this WTA network: the center-surround response profile was obtained by stimulating the central cell of the network with a constant input current, for a fixed value of V_{ex} and different values of V_{inh}.

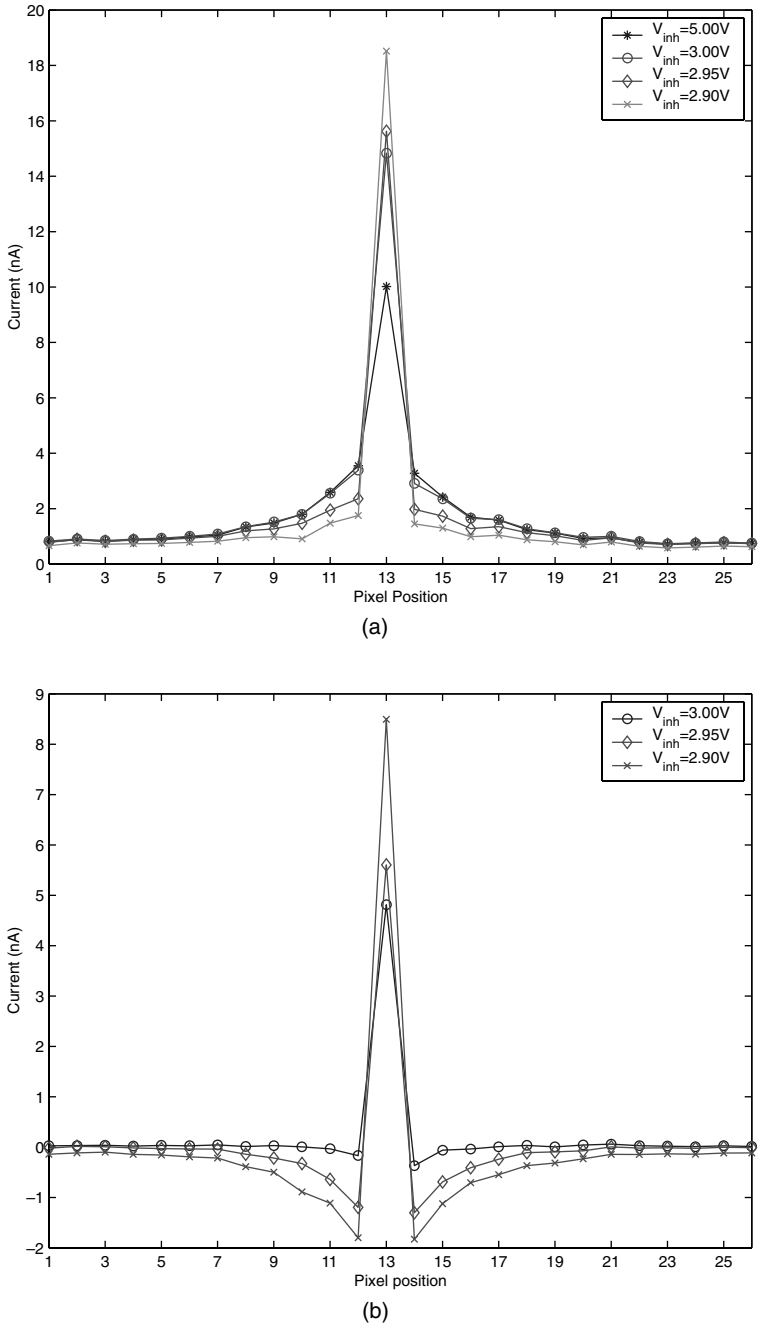

Fig. 7. Response of the hysteretic WTA network to a single pixel input (pixel 13, with $V_{gs,13} = 1.1$ V) for a fixed value of $V_{ex} = 1.825$ V. (a) Current output for 4 different values of V_{inh}. (b) Relative difference between output of the network with global inhibition ($V_{inh} = 5$ V) and output of the network with 3 different values of V_{inh}.

4. Applications

Besides being a practical, compact, low-power circuit for generic applications that require a winner-take-all type of computation, the circuit proposed in this paper is particularly useful in all those applications that involve the processing of sensory signals and the selection of one or more inputs (e.g., for determining

motor actions in a sensory-motor system). The center-surround response profile of the network shown in Fig. 7 is a rough approximation of a difference of two Gaussians (DOG), which in turn approximates closely a Laplacian of a Gaussian $\nabla^2 G$. It has been argued that this type of operator is ideal for detecting intensity changes in sensory stimuli [24] and resembles closely the response profile of many types of neurons, ranging from simple cells in the visual cortex of mammals [25] to cells in the somatosensory cortex of rats [26], to neurons in the midbrain of barn owls [27]. Examples of applications that exploit the local excitatory feedback and distributed hysteresis circuits described in Sections 2.1 and 3.1 include visual tracking of targets whose images shift smoothly from one pixel to the next [19,28]. Another example of an application that exploits the center-surround response properties of the hysteretic WTA network is given by multi-chip selective attention systems such as the one described in [29]. In these kinds of systems, sensory signals generated by silicon retinas [30], silicon cochleas [31] and other types of neuromorphic sensors are sent to a WTA network, which is then used to select one or more inputs, corresponding to the most salient input. Selective attention systems that use this kind of WTA network could thus be used for optimizing the allocation of computational resources by selectively processing only the regions in the sensory space that lie in the immediate neighborhood of the selected location and neglecting all other regions.

5. Conclusions

We presented an extension of the current-mode WTA circuit originally proposed in [1], adding local excitatory feedback, diode-source degeneration, lateral excitatory coupling and lateral inhibitory coupling. Although some of the extensions presented have already been proposed in the past, the circuit described in this article is the first one to implement all of them in the same circuit. We described the functional relevance of the enhancements proposed and derived analytically the dependence of the lateral coupling on the circuit parameters. We designed and fabricated a CMOS VLSI chip containing both the classical WTA network and the enhanced WTA network "back-to-back," in order to perform an accurate comparison between the two circuits. We characterized the circuits and presented experimental data to show the behavior of the implemented WTA networks. As demonstrated in the previous sections, the circuits proposed are suitable for integration into analog VLSI neuromorphic systems.

Acknowledgments

This work was supported by the Swiss National Science Foundation SPP Grant and the U.S. Office of Naval Research. Fabrication of the integrated circuits was provided by MOSIS.

References

1. Lazzaro, J., Ryckebusch, S., Mahowald, M. A. and Mead, C. A., "Winner-take-all networks of $O(n)$ complexity." In *Advances in neural information processing systems,* D. S. Touretzky, Ed., San Mateo—CA, 1989, 2, pp. 703–711, Morgan Kaufmann.
2. Nakada, A., Konda, M., Morimoto, T., Yonezawa, T., Shibata, T. and Ohmi, T., "Fully-parallel VLSI implementation of vector quantization processor using neuron-MOS technology." *IEICE Trans. on Electron.* E82C(9), pp. 1730–1738, September 1999.
3. Yu, H. M., Miyaoka, R. S. and Lewellen, T. K., "A high-speed and high-precision winner-select-output (WSO) ASIC." *IEEE Trans. on Nucl. Sci.* 45(3), pp. 772–776, June 1998.
4. Demosthenous, A., Smedley, S. and Taylor, J., "A CMOS analog winner-take-all network for large-scale applications." *IEEE Trans. on Circuits and Systems I* 45(3), pp. 300–304, March 1998.
5. Lau, K. T. and Lee, S. T., "A CMOS winner-takes-all circuit for self-organizing neural networks." *Int. J. Electron.* 84(2), pp. 131–136, February 1998.
6. Meador, J. L. and Hylander, P. D., "Pulse coded winner-take-all networks." In *Silicon Implementation of Pulse Coded Neural Networks,* M. E. Zaghloul, J. L. Meador and R. W. Newcomb, Eds., Chapter 5, pp. 79–99. Kluwer, 1994.
7. ElMasry, E. I., Yang, H. K. and Yakout, M. A., "Implementations of artificial neural networks using current-mode pulse width modulation technique." *IEEE Trans. Neural Netw.* 8(3), pp. 532–548, May 1997.
8. Serrano, T. and Linares-Barranco, B., "A modular current-mode high-precision winner-take-all circuit." *IEEE Trans. on Circuits and Systems II* 42(2), pp. 132–134, February 1995.
9. He, Y. and Sanchezsinencio, E., "Min-net winner-take-all CMOS implementation." *Electron. Lett.* 29(14), pp. 3, July 1993.
10. Choi, J. and Sheu, B. J., "A high-precision VLSI winner-take-all circuit for self-organizing neural networks." *IEEE J. Solid-State Circuit* 28(5), pp. 576–584, May 1993.
11. Lazzaro, J. and Mead, C., "A silicon model of auditory localization." *Neural Computation* 1, pp. 41–70, 1989.
12. Horiuchi, T., Bair, W., Bishofberger, B., Lazzaro, J. and Koch, C., "Computing motion using analog VLSI chips: an experimental comparison among different approaches." *International Journal of Computer Vision* 8, pp. 203–216, 1992.
13. DeWeerth, S. P. and Morris, T. G., "Analog VLSI circuits for primitive sensory attention." In *Proc. IEEE Int. Symp. Circuits and Systems.* IEEE 6, pp. 507–510, 1994.

14. Starzyk, J. A. and Fang, X., "CMOS current mode winner-take-all circuit with both excitatory and inhibitory feedback." *Electronic Letters* 29(10), pp. 908–910, May 1993.
15. DeWeerth, S. P. and Morris, T. G., "CMOS current mode winner-take-all circuit with distributed hysteresis." *Electronics Letters* 31(13), pp. 1051–1053, June 1995.
16. Indiveri, G., "Winner-take-all networks with lateral excitation." *Jour. of Analog Integrated Circuits and Signal Processing* 13(1/2), pp. 185–193, 1997.
17. Morris, T. G. and DeWeerth, S. P., "Analog VLSI excitatory feedback circuits for attentional shifts and tracking." *Analog Integrated Circuits and Signal Processing* 13(1/2), pp. 79–92, May/June 1997.
18. Horiuchi, T. and Niebur, E., "Conjunction search using a 1-D, analog VLSI-based attentional search/tracking chip." In *Confference for Advanced Research in VLSI,* D. Scott Wills and Stephen P. DeWeerth, Eds., pp. 276–290. IEEE Computer Society, 1999.
19. Indiveri, G., "Neuromorphic analog VLSI sensor for visual tracking: Circuits and application examples." *IEEE Trans. on Circuits and Systems II* 46(11), pp. 1337–1347, November 1999.
20. Boahen, K. A. and Andreou, A. G., "A contrast sensitive silicon retina with reciprocal synapses." In *Advances in neural information processing systems,* D. S. Touretzky, M. C. Mozer and M. E. Hasselmo, Eds., IEEE, 1992, vol. 4, MIT Press.
21. Vittoz, E. A. and Arreguit, X., "Linear networks based on transistors." *Electronics Letters* 29(3), pp. 297–298, February 1993.
22. Mead, C. A., "Neuromorphic electronic systems." *Proceedings of the IEEE* 78(10), pp. 1629–1636, 1990.
23. Gray, P. M. and Meyer, R. G., *Analysis and Design of Analog Integrated Circuits,* Wiley, second edition, 1984.
24. Marr, D., *Vision, a Computational Investigation into the Human Representation & Processing of Visual Information,* Freeman, San Francisco, 1982.
25. Jones, J. and Palmer, L., "The two-dimensional spatial structure of simple receptive fields in cat striate cortex." *J. Neurosci.* 58, pp. 1187–1211, 1987.
26. Moore, C. I., Nelson, S. B. and Sur, M., "Dynamics of neuronal processing in rat somatosensory cortex." *Trends Neurosci.* 22(11), pp. 513–520, November 1999.
27. Knudsen, E. I. and Konishi, M., "Center-surround organization of auditory receptive fields in the owl." *Science* 202(4369), pp. 778–780, November 1978.
28. Indiveri, G., Kramer, J. and Koch, C., "System implementations of analog VLSI velocity sensors." *IEEE Micro* 16(5), pp. 40–49, October 1996.
29. Indiveri, G., "Modeling selective attention using a neuromorphic analog VLSI device." *Neural Computation* 12(12), pp. 2857–2880, December 2000.
30. Boahen, K. A., "A retinomorphic vision system." *IEEE Micro* 16(5), pp. 30–39, October 1996.
31. Fragnière, E., van Schaik, A. and Vittoz, E., "Design of an analogue VLSI model of an active cochlea." *Jour. of Analog Integrated Circuits and Signal Processing* 13(1/2), pp. 19–35, May 1997.

Giacomo Indiveri is a Research Assistant at the Institute of Neuroinformatics (INI) of the Swiss Federal Institute and the University of Zurich. Before joining the INI, from 1994 to 1996, he worked as a Postdoctoral Fellow in the Department of Biology of the California Institute of Technology, with Prof. C. Koch, on the design of analog VLSI subthreshold neuromorphic architectures for low-level visual tasks and motion detection. His current research interests include the design and implementation of neuromorphic systems for modeling selective attention neural mechanisms, and for exploring the computational properties of networks of silicon integrate and fire neurons. Indiveri is co-teacher of two classes on the analysis and design of analog VLSI Neuromorphic Systems at the Swiss Federal Institute of Zurich and co-organizer of the Workshop on Neuromorphic Engineering, held annualy in Telluride, Colorado.